EUROPEAN ORGANIZATION FOR NUCLEAR RESEARCH
ORGANISATION EUROPEENNE POUR LA RECHERCHE NUCLEAIRE

CERN - PS DIVISION

PS/BD/Note 2000-002

DUOPLASMATRON SOURCE TRANSVERSE PROFILE MEASUREMENT

Y. Bilinsky, E. Chevallay, R. Maccaferri, V. Prieto.

Abstract

This paper describes transverse profile measurements made on the duoplasmatron source.
The detector itself consists of a microchannel plate (MCP) followed by a phosphor. The phosphor image is recorded by a CCD camera.
The advantages and drawbacks are discussed, as well as the experimental results obtained by comparison with other detectors installed in the same beam line

Geneva, Switzerland
29 May 2000

1. INTRODUCTION

A microchannel plate (MCP) is a secondary-electron multiplier which detects and amplifies electrons in two-dimensions. The MCP is sensitive not only to electrons but to ions, vacuum ultraviolet light, X-rays and Gamma-rays, making it useful in a wide range of detection applications. In our case, the MCP was used to measure the transverse profiles of the Duoplasmatron source (protons, 50keV), in comparison with a Secondary Emission monitor (SEM). A Faraday Cup aimed to measure the proton beam intensity was installed in the same beam line.

2. THE MCP.

The MCP [ref.1] consists of a lead glass plate perforated by an array of microscopic channels (in our case with 25μm diameter) oriented parallel to one another. The inner surfaces of the channels are treated with a semiconductor material so as to act as secondary electron emitters while the flat end surfaces of the plate are coated with a metallic alloy so as to allow a potential difference to be applied along the length of the holes. Electrons entering a channel are thus accelerated along the hole until they eventually strike the wall to release further electrons which, in turn, are accelerated and so on. Each channel thus acts as a continuous dynode. Typical microchannel plates have from 10^4-10^7 holes and can provide multiplication factors of 10^3-10^4. Typical detection efficiency for protons at 50keV [ref.2]is about 0.7. Figures 1.1 and 1.2 show the gain of our MCP and its technical parameters, [ref .3]. We use a single stage MCP.

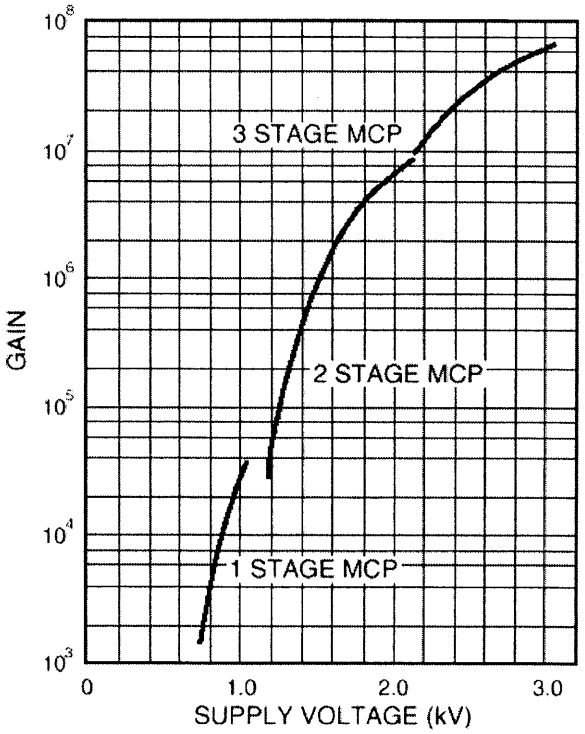

Fig. 1.1

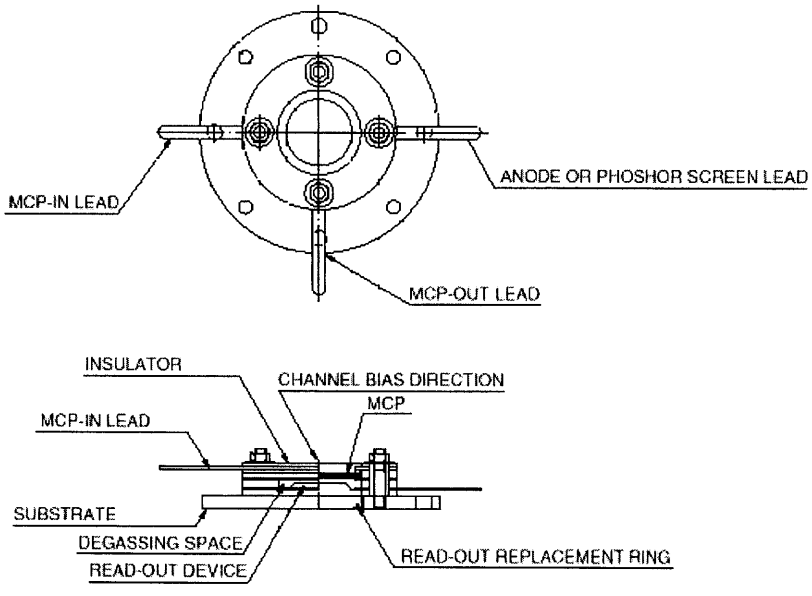

Fig. 1.2

Figure 1.1: Typical gain dependence on the applied bias voltage(taken from [ref.3]).
Figure 1.2. : Single stage MCP assembly outline.

Figure 2 shows the general detection efficiency for MCP's

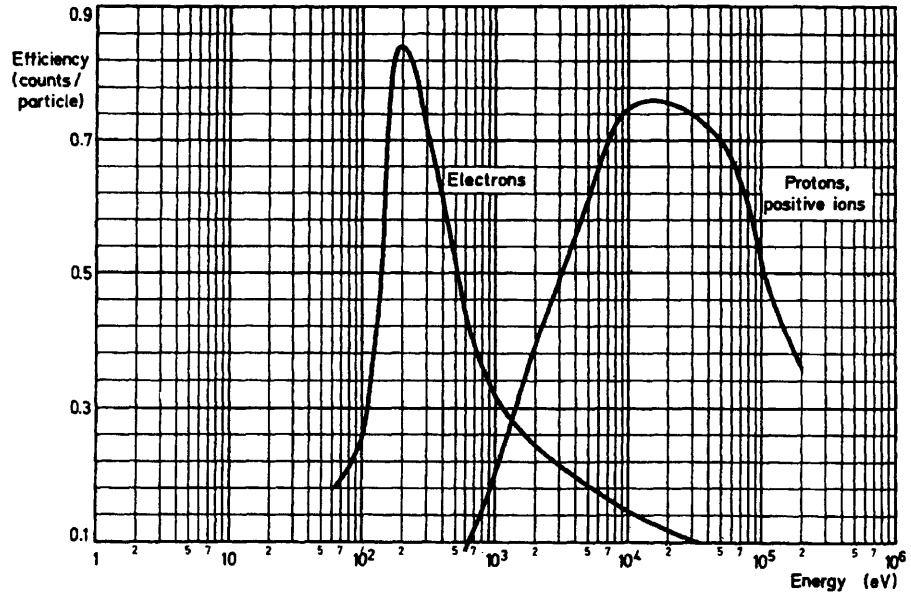

Figure 2. Typical detection efficiencies for electrons protons and positive ions.(taken from [ref.2])

The read-out device of the MCP is a Phosphor screen (of P20 type) . Figure 3 shows the assembly of our MCP.

Table 1 shows the general specifications of our used single stage MCP assembly.

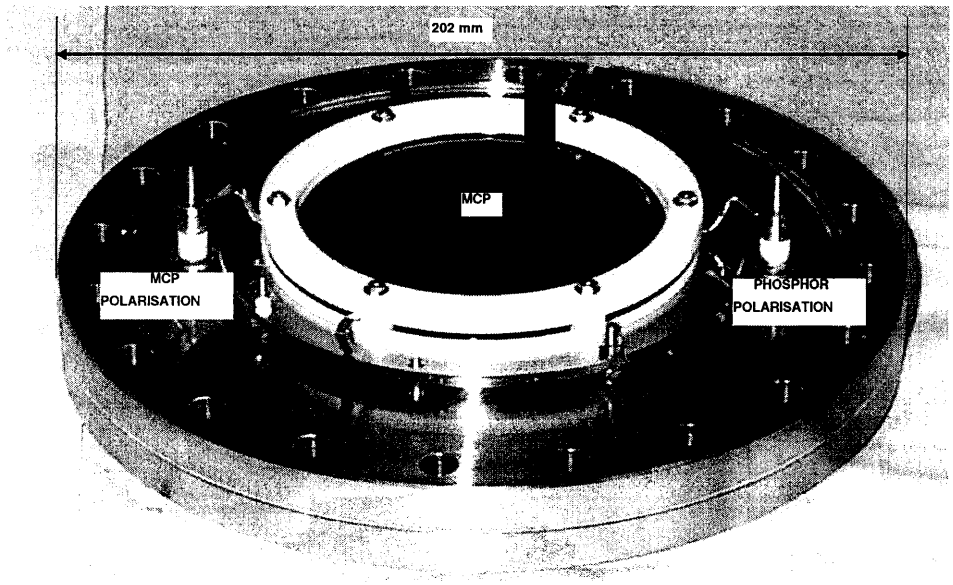

Figure 3. MCP Assembly.

Gain(max)	*MCP Supply Voltage*	*Voltage between the MCP output and the phosphor.*
$4*10^4$	1kV	4kV

Table 1. General specifications of MCP assembly F2226-14P(Hamamatsu Photonics).

3. THE BEAM LINE.

Figure 4 shows the Duoplasmatron source beam line lay-out.

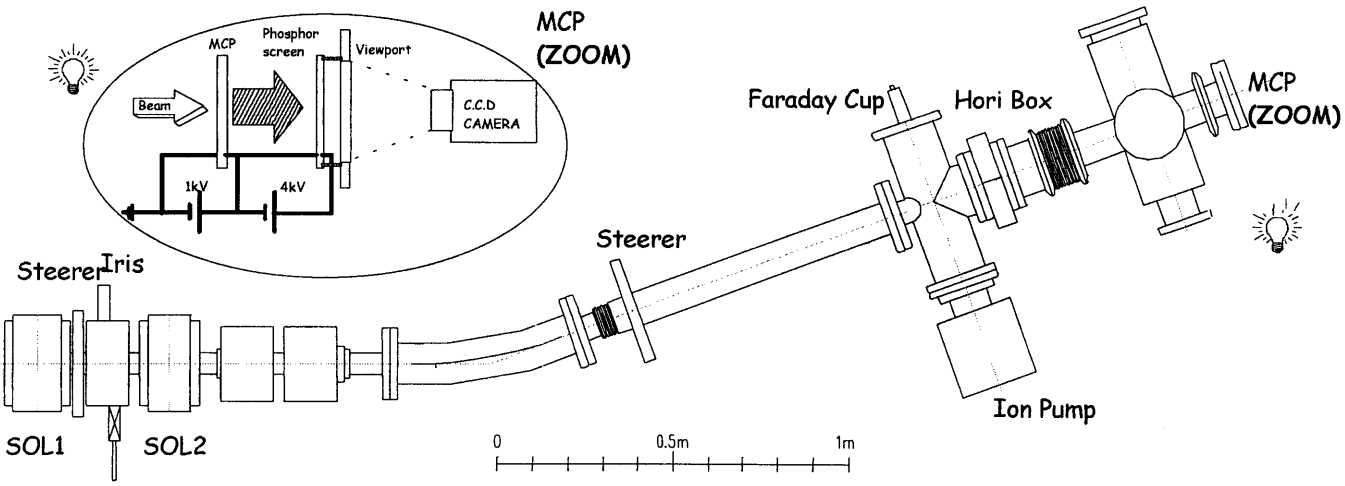

Figure 4. Diagram of the beam line (ADRFQ37)

The MCP- Phosphor assembly is placed at the end of the line at vacuum pressure lower than 10^{-6} torr. Upstream our monitor two detectors are placed, namely a Faraday Cup and a SEM (named later on "Hori-box"). The SEM and its associate software provides us the proton beam distribution and center of gravity and therefore a way of comparison.
The Faraday cup measures the total charge which penetrates it. With this detector we took some measurements in order to determine the intensity range of our system.

3.1 . The SEM (Hori-box).

The Hori-box is a S.E.M (Secondary Emission Monitor) placed in the beam line as shown in Figure 3. This detector is made of 32 wires (tungsten gold-plated, ∅10μm) per plane. Its resolution is 1 mm. The upper current limit is about 50nA/cm^2 in 5μs, and its lower limit is not defined yet. [ref. 4].
The associated software acquires the data of each wire and provides the transverse profile on a screen. In this way the beam position can be determined with an accuracy of 1mm. In addition, the center of gravity coordinates, are computed.

3.2. The Faraday Cup.

A Faraday cup is essentially a metal collector stopping all the particles which penetrate it. Coupled to an integrator or an amplifier current we are able to determine the number of incident particles or the beam intensity.
The particles stopped by the collector will create low energy (to the order of a few 10eV) secondary electrons. These electrons will have the tendency to leave the detector and as a

matter of fact will alter the measurement. It is thus necessary to place, upstream from the target, a negatively polarized electrode in order to repel the secondary electrons.[ref. 5]

4. THE ACQUISITION SYSTEM.

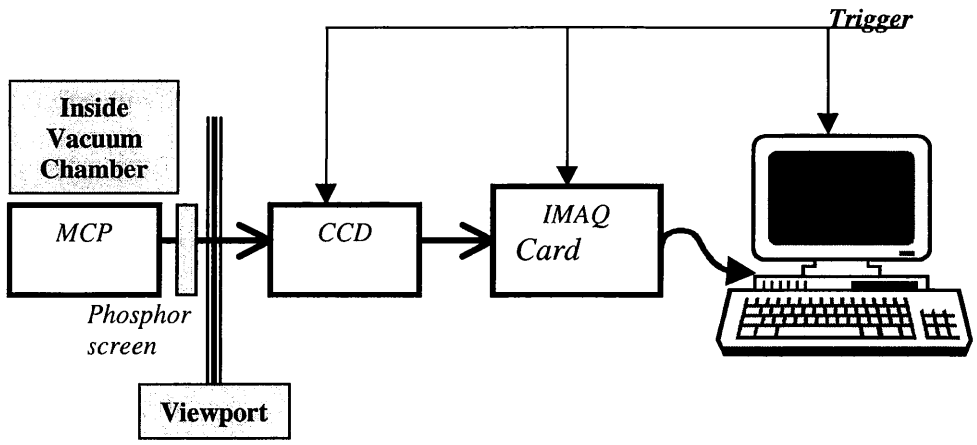

Figure 5. Block diagram of the acquisition system.

A block diagram of the computerized system is shown in Figure 5.
The phosphor image is processed by the CCD camera and memorized in the computer using an IMAQ-Card controlled with a Labview application program. The whole system is synchronized using a trigger signal from the duoplasmatron source.
The IMAQ-Card digitalizes the image as seen by the CCD. From the stored data the program provides a spot-like display and evaluates the horizontal and vertical transverse distributions or profiles. An example of an image and its transverse profiles, (Vertical and horizontal) is represented by Figure 6.1 and Figures 6.2, 6.3, respectively.

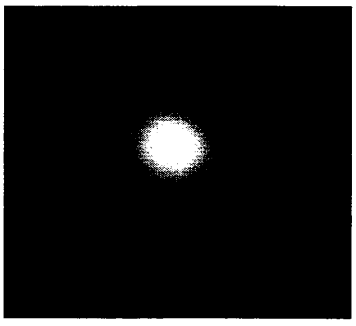

Figure 6.1. View of a Low intensity beam. (30nA,6μs, 50keV). U_{MCP}= 630V, $U_{phosphor}$ = 3kV. (bmp file take with Labview).

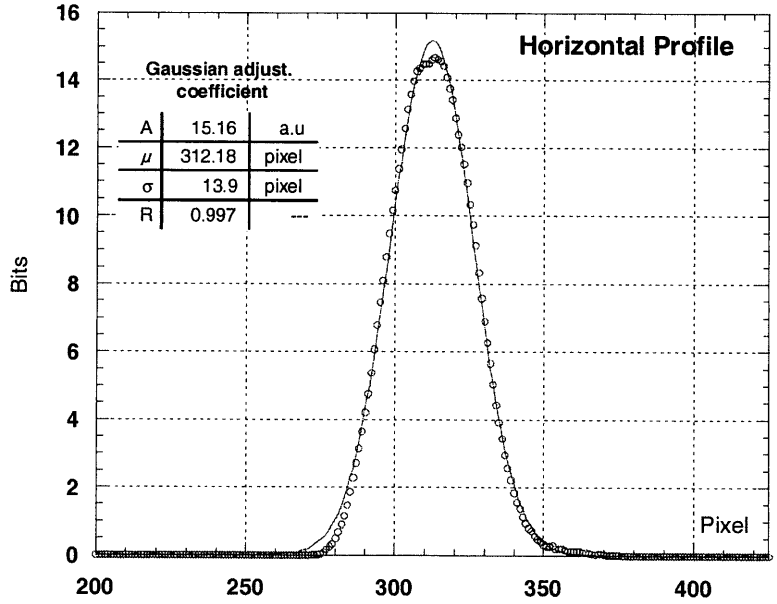

Figure 6.2. View of the Horizontal Beam profile taken from Figure 6.1.

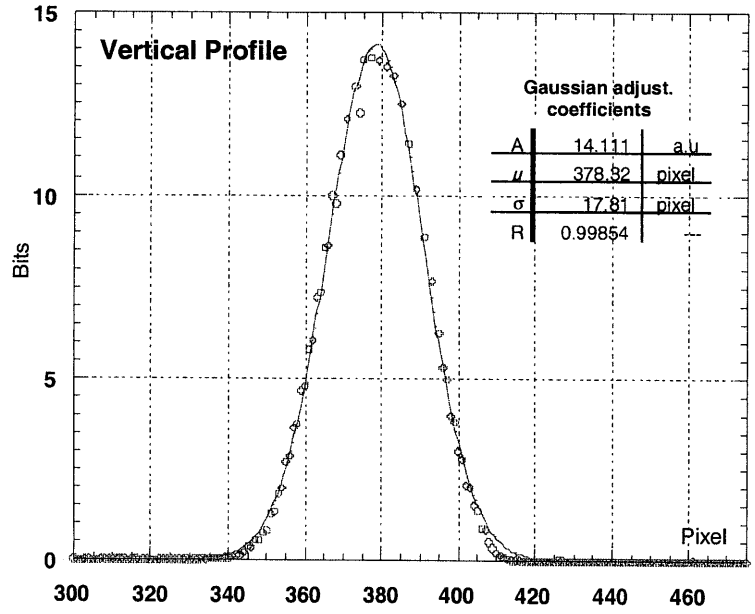

Figure 6.3. View of the vertical Beam profile taken from Figure 6.1.

As we can see from Figures 6.2 and 6.3, the distribution are nearly Gaussian as confirmed by their form and by:

$$F(y)= A \exp [-(y-\mu)^2/2\sigma^2]$$

Where y, μ and σ are expressed in pixel and A in number of bits. However these coefficients are given in a separate box for each transverse profile measurement.

The resolution is quite good. The intensity can be reduced by a factor 3, without any further action on the MCP gain.

5. MEASUREMENTS AND RESULTS.

The first type of measurement was made in order to compare our data with regard to those obtained from the Hori-Box. The second type of measurement was made in conjunction with the Faraday Cup in order to determine the MCP lower intensity limit.

5.1. Comparison Hori box – MCP

The SEM was introduced into the beam and the center of gravity coordinates (in horizontal and vertical planes) were recorded for both the Hori-box (in mm) and the MCP+Phosphor (in pixel). The measurements are represented graphically (Figure 7.1, 7.2) and the regression lines calculated. Two other lines are drawn which correspond to the error in the constant term (one corresponds to a+da and the other to a-da) of the regression line.
As we can see, the linearity of our system is quite good. (since the correlation factor R^2= 0.9992 for the vertical plane and R^2=0.9971 for the horizontal plane). The error in the constant term "a", in the horizontal plane is higher than in the vertical plane da(vert)= 0.309, da(hor.)= 0.780). The reason can be attributed to the fact that the Hori box had two broken wires in the horizontal plane and it is therefore reasonable to suppose that the measurements in this plane are less accurate.

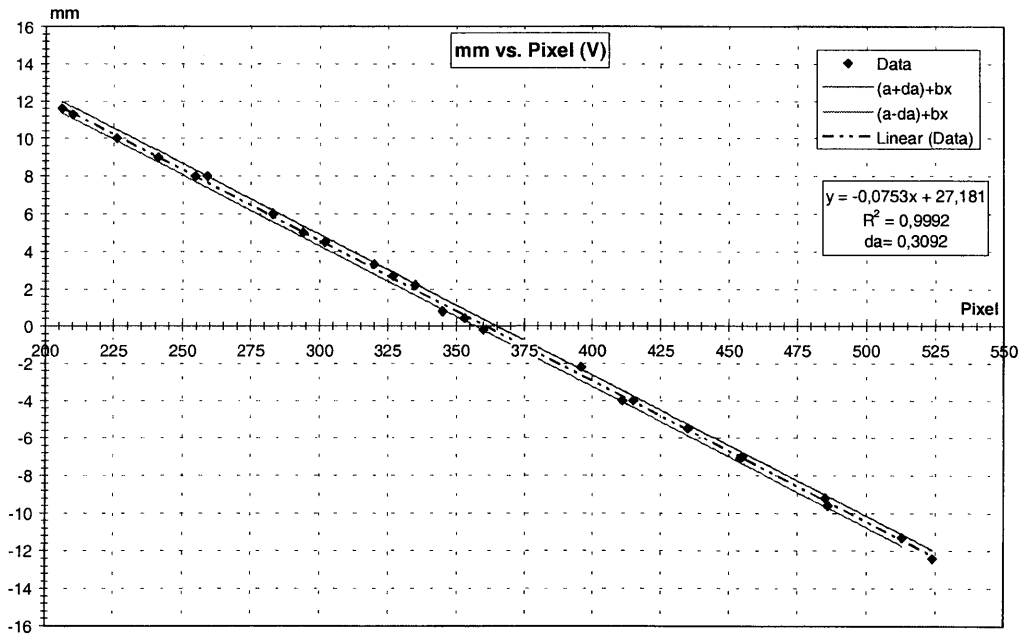

Figure 7.1. Hori-box position (in mm) vs. MCP position (in pixel). Vertical Plane

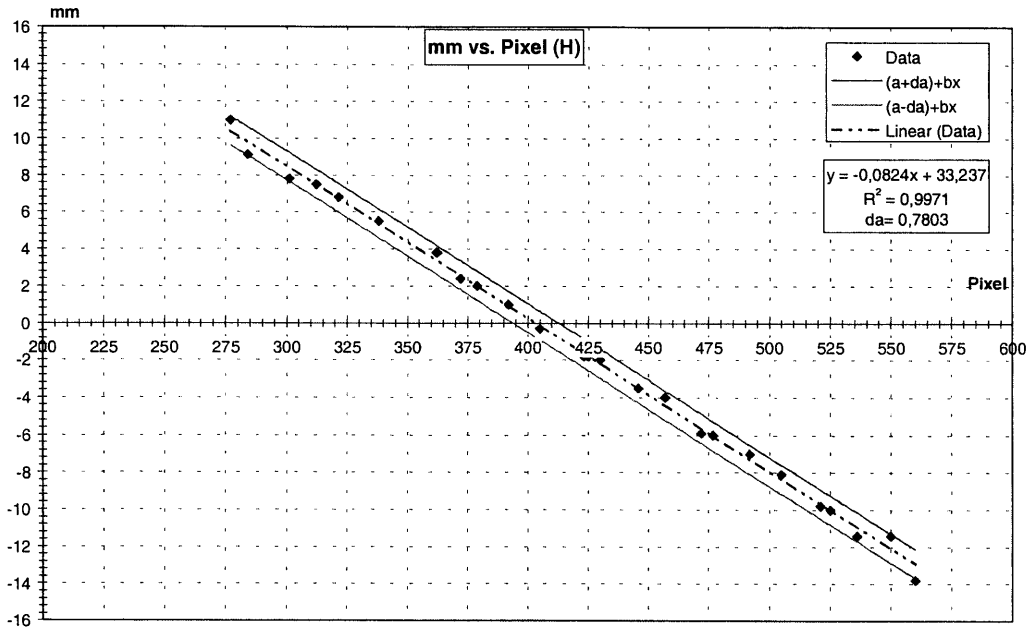

Figure 7.2. Hori-box position (in mm) vs. MCP position (in pixel). Horizontal Plane.

If we calculate the relation between a given displacement Δy recorded in the Hori Box and the corresponding Δx as seen by the CCD camera, we find:
Δy=1mm corresponds to Δx= 13 pixels in the vertical plane (76μm per pixel)
Δy= 1mm corresponds to Δx= 12 pixels in the horizontal plane. (83μm per pixel)

Other measurement have shown, due to the steering elements, a magnification factor between the Hori grid and the phosphor. In the horizontal plane the width on the phosphor is 1.447 times larger than that on the Hori device, while in the vertical plane the width on the phosphor is 1.612 times larger than that measured on the Hori monitor.

5.2 Comparison Faraday Cup-MCP.

As mentioned before, a second type measurement was made with the MCP in order to find a lower intensity limit for our device. The intensity was measured by the Faraday Cup.
The Faraday Cup was polarized at –150V so as to be sure that all secondary electrons are collected by the cup.
Figures 8.1, 8.2 and 8.3 show the results obtained for a 400nA intensity (duration Δt=6,6μs, Energy 50keV, protons) .

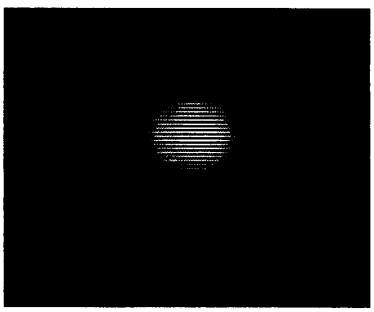

Figure 8.1. Spot for a beam proton intensity of 400nA

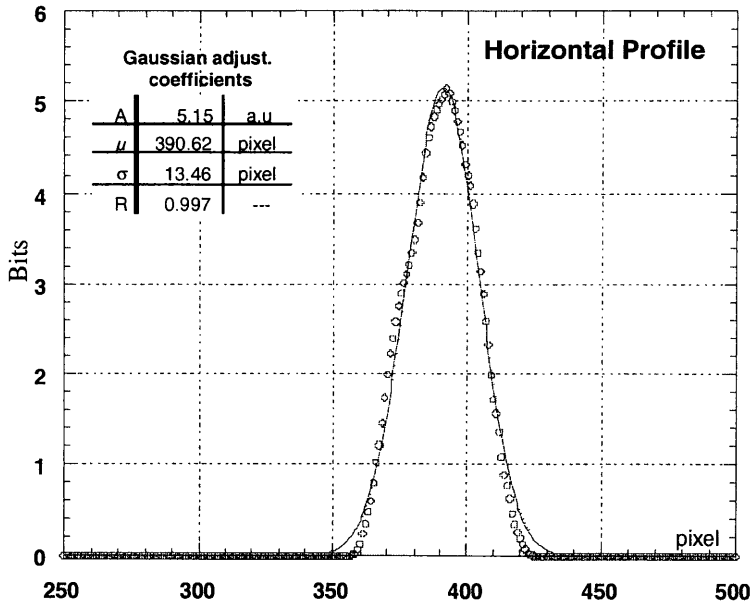

Figure 8.2. Horizontal beam profile taken from Figure 8.1

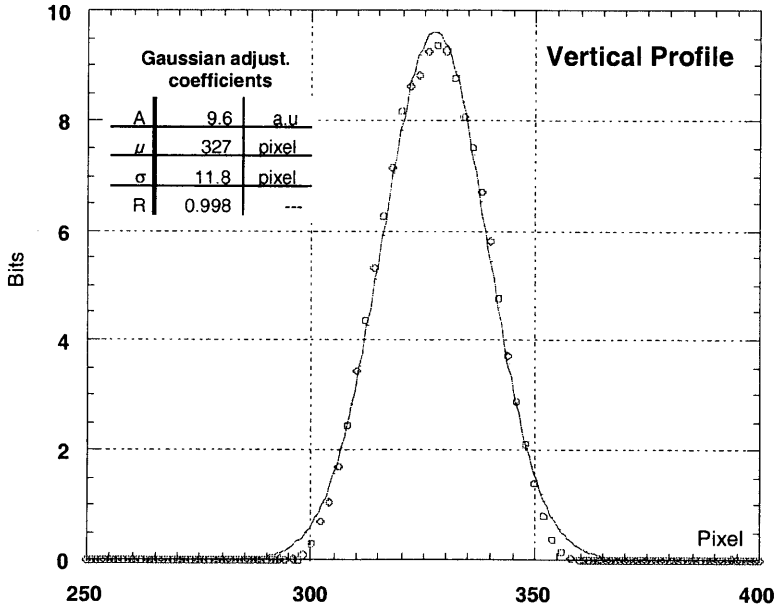

Figure 8.3. Vertical beam profile taken from Figure 8.1.

The detector parameters are, for this case:
U_{MCP} = 510V
$U_{Phos.}$ = 3,5Kv
Figures 9.1, 9.2 and 9.3 give the results for a 4nA proton beam (Δt= 6,6μs, 50keV).

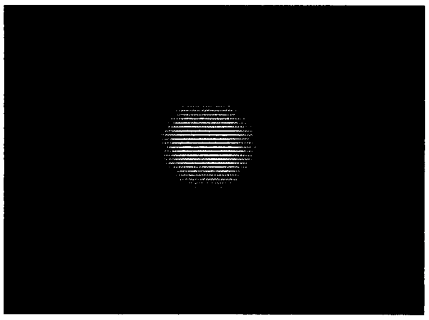

Figure 9.1. Spot for an intensity of 4nA

The detector parameters are, for the profiles represented by Figure 9:

U_{MCP} = 710V
$U_{Phos.}$ = 3,5kV

It is clear that the MCP based detector accuracy is quite good within a large range of intensities. Different intensities are probed by different MCP gain adjustments.

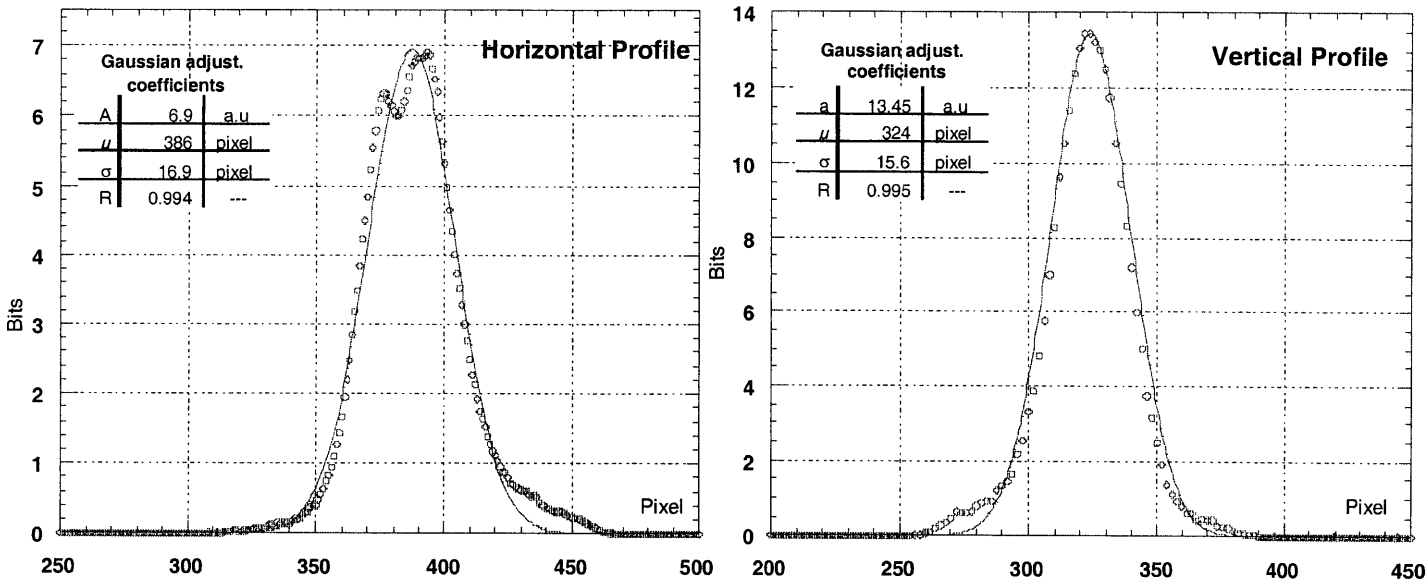

Figure 9.2. Horizontal beam profile taken from Figure 9.1
Figure 9.3. Vertical beam profile taken from Figure 9.1.

5.3. Linearity measurements.

To conclude our measurements of the MCP we made linearity tests. For that purpose we maintained the MCP and "Phosphor" voltage constant and varied the incident proton intensity. The resulting "profile-pixel" are then summed horizontally and vertically. Table 2 shows the raw results which are plotted in Figure 10 with the regression line.

Incident Charge (pC)	***ΣHorizontal (bits)***	***ΣVertical (bits)***
2	635	522
3.4	1371	1128
4	1468	1208

Table 2. Measurements with fixed gain on the MCP

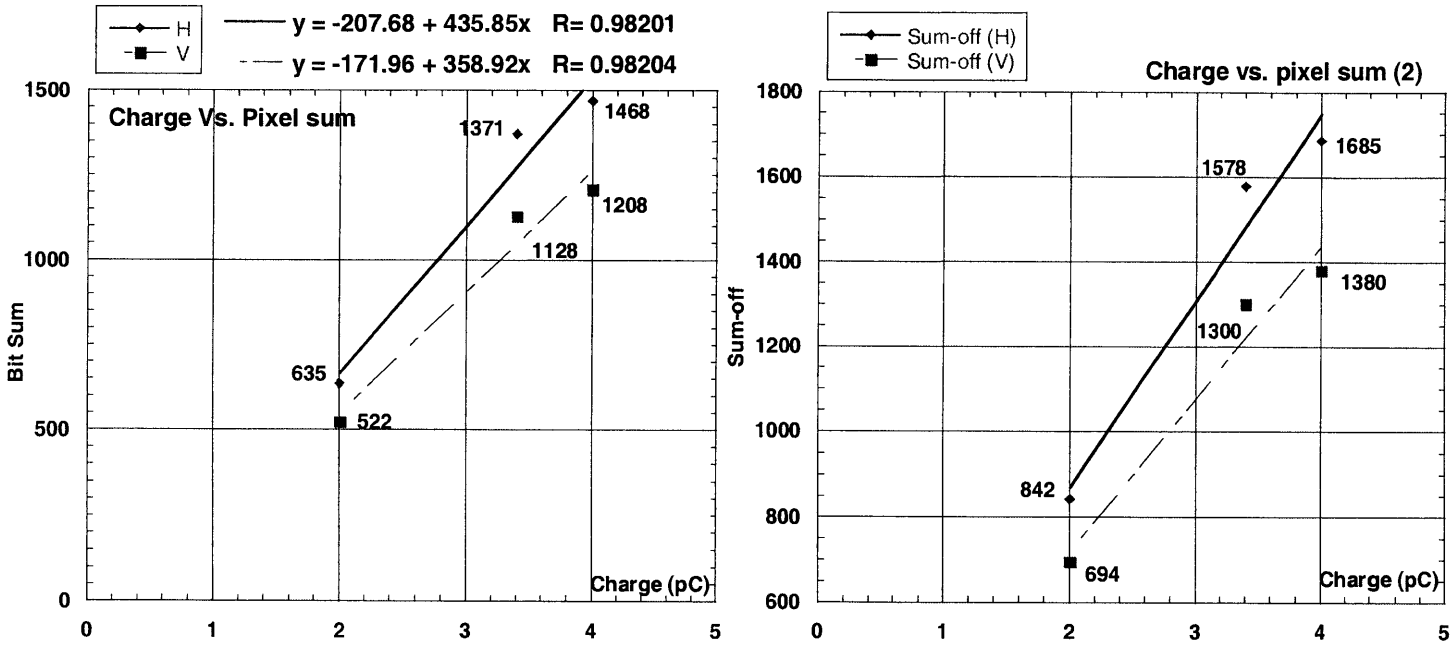

Figure 10. Bit Sum versus incident charge.(for a fixed gain on the MCP)
Figure 11. Bit Sum versus incident charge, without offset .

As we can observe from the plot and table, once the offset is algebraically subtracted from the regression line, the response is almost linear (see Figure 11) provided that the phosphor was not saturate. The difference in the "x" coefficients, between both planes, results from the fact that the number of pixels are not the same (700 in the Horizontal and 576 in the vertical plane)

6. CONCLUSIONS.

The described monitor (MCP+ Phosphor + CCD) is well suited to measure the transverse rms dimensions and position of low intensity (less than 1μA) and low energy (less than 100keV) ion beam as used in sources.
The detector itself needs modest vacuum conditions (pressures $\leq 10^{-6}$ torr.) as is expected to be used at the end of the beam line.

References

[ref.1] W.R. Leo. Techniques for nuclear and Particle Physics experiments. A How to approach. 2nd.Edition (p 183) Springer-Verlag Ed. 1994.

[ref.2] Phillips Data handbook. Electron Tubes. Book T9, 1985 (p.311).

[ref.3] Hamamatsu Photonics K.K, MCP Assembly selection guide. 1996.

[ref.4] Private communication, Mr. Hori.

[ref.5] G. Molinari,V. Prieto. Test d'une coupe de Faraday avec la source duoplasmatron. PS/BD/ Note 2000-01.

Liste de Distribution:

Groupe PS/BD :

ANGOLETTA Maria Elena	L03200
BAL Cathelijne	L03010
BELLEMAN Jeroen	G03010
BERTRAND Jean-Claude	J03720
BOSSER Jacques	L07210
BOUDOT Robert	G03200
BRAVIN Enrico	L03200
CARTER Colin	G02600
CHOHAN Vinod	L08100
DAMIANI Michel	G03110
D'AMICO Tommaso	L20300
DESCHAMPS Stéphane	L07810
DIGONZELLI Jean-Marc	G03010
DIMOPOULOU Christina	L07810
DURAND Jacques	L18710
DUTRIAT Christian	L03600
FOCKER Gerrit	J03720
FRØYSLAND Tom	G03010
GALMANT Catherine	L08610
GIUDICI François	L04210
GONZALEZ José	G02810
GUILLAUME Jean	L03100
LE GRAS Marc	G03110
LENARDON Franco	G03210
LONGO Salvatore	G03310
LUDWIG Michael	L08700
MACCAFERRI Remo	L07510
MARQVERSEN Ole	G02700
MARTINI Gérard	L03010
MOLINARI Gianni	L07600
ODIER Patrick	G02900
OLSFORS Jan	L18110
PERRIOLLAT Fabien	L19800
PLUM Michael	L08900
POTIER Jean-Pierre	L19510
PRIETO Virginia	L07200
QUENOUILLERE Rémi	L09800
RAICH Ulrich	L18100
RENAUD Yves	L09800
SAID Emmanuel	L02610
SAUTIER Roland	L02600
SCHNELL Jean-Denis	G02910
SOBY Lars	G02800
THOMI Jean-Claude	L09000
TIRARD Serge	G02500
TOEPFFER Christian	L07000
TRANQUILLE Gérard	L06520
WILLIAMS David John	G02510

Groupe SI/BI :

BARIBAUD Guy	Y04710
DEHNING Bernd	Y02500
GRAS Jean-Jacques	Y04920
JUNG Roland	Z13500
SCHMICKLER Hermann	Y02200

Division PS :

HILL Charles	L03510
LOMBARDI Alessandra	L03700
PIRKL Werner	L03110